JACS
JOURNAL OF THE AMERICAN CHEMICAL SOCIETY
Article
pubs.acs.org/JACS

Cations Bind Only Weakly to Amides in Aqueous Solutions

Halil I. Okur, Jaibir Kherb, and Paul S. Cremer*

Department of Chemistry, Texas A&M University, College Station, Texas 77843, United States

Supporting Information

ABSTRACT: We investigated salt interactions with butyramide as a simple mimic of cation interactions with protein backbones. The experiments were performed in aqueous metal chloride solutions using two spectroscopic techniques. In the first, which provided information about contact pair formation, the response of the amide I band to the nature and concentration of salt was monitored in bulk aqueous solutions via attenuated total reflection Fourier transform infrared spectroscopy. It was found that molar concentrations of well-hydrated metal cations (Ca^{2+}, Mg^{2+}, Li^{+}) led to the rise of a peak assigned to metal cation-bound amides (1645 cm^{-1}) and a decrease in the peak associated with purely water-bound amides (1620 cm^{-1}). In a complementary set of experiments, the effect of cation identity and concentration was investigated at the air/butyramide/water interface via vibrational sum frequency spectroscopy. In these studies, metal ion−amide binding led to the ordering of the adjacent water layer. Such experiments were sensitive to the interfacial partitioning of cations in either a contact pair with the amide or as a solvent separated pair. In both experiments, the ordering of the interactions of the cations was: $Ca^{2+} > Mg^{2+} > Li^{+} > Na^{+} \approx K^{+}$. This is a direct cationic Hofmeister series. Even for Ca^{2+}, however, the apparent equilibrium dissociation constant of the cation with the amide carbonyl oxygen was no tighter than ∼8.5 M. For Na^{+} and K^{+}, no evidence was found for any binding. As such, the interactions of metal cations with amides are far weaker than the analogous binding of weakly hydrated anions.

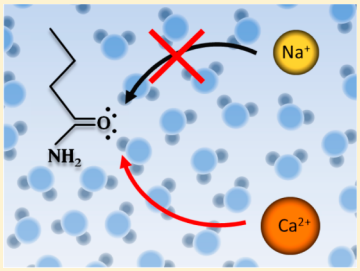

INTRODUCTION

The effects of inorganic salts on proteins and macromolecules in aqueous solutions generally follow a Hofmeister series, as first reported in 1888.[1−5] The series was traditionally ranked according to the ability of each salt to precipitate proteins from aqueous solutions.[1] The series for anions is typically: $CO_3^{2-} > SO_4^{2-} > H_2PO_4^{-} > F^{-} > Cl^{-} > NO_3^{-} > Br^{-} > I^{-} > SCN^{-} > ClO_4^{-}$. Anions to the left of chloride are strongly hydrated and lead to greater salting-out behavior, while ions to the right are weakly hydrated and salt proteins into solution in the direct Hofmeister series. Chloride is often found to be the dividing point between salting-in and salting-out behavior in the series. By contrast to anions, the Hofmeister effect for cations is usually weaker.[6] The series for uncharged systems like peptide backbones is typically:[7]

$$N(CH_3)_4^{+} > NH_4^{+} > Cs^{+} > Rb^{+} > K^{+} > Na^{+} > Li^{+} > Ca^{2+} > Mg^{2+}$$

Again, ions on the left salt neutral proteins/macromolecules out of solution, while ions on the right lead to salting-in behavior. Curiously, the most effective cations for salting proteins into solution are the ones that are most strongly hydrated, while cations that are weakly hydrated lead to salting-out behavior. This is opposite of the anion series. Moreover, despite being less pronounced than the anion series, specific cation effects have direct importance for protein folding, protein−protein interactions, cell signaling, protein aggregation, enzyme catalysis, and even biotechnology.[4,6,8−10] Thus, quantifying cation interactions with amide moieties and polypeptide backbones is of great fundamental importance.

The binding site for anions with polypeptide backbones has been shown to involve a combination of the polar nitrogen atom and the adjacent hydrocarbon group.[11] The interactions of cations with the peptide backbone have been difficult to measure directly in aqueous solutions due to the interference of side chain and secondary structure effects.[12−14] Nevertheless, the binding site for cations should involve the carbonyl oxygen of the amide.[15] However, it has been a particular challenge to obtain quantitative binding constant information for metal cations with amide moieties. There are a few structural studies in the literature focusing on amide−cation interactions in nonaqueous media[16,17] and in the solid phase.[18] Five decades ago, Bello and co-workers reported qualitative association of Li^{+} and Ca^{2+} with the simple amide-containing compounds, *N*-methyl acetamide (NMA) and *N*,*N* dimethyl acetamide, at very high concentrations of the organic molecule in aqueous solutions by viscosity and calorimetric methods.[18−20] In the solid state, these same authors found adducts between cations and amide-containing molecules by X-ray crystallography. Later, Robinson and co-workers attempted to study cation and anion association with end-capped mono, di, tri, and tetraglycine molecules by solubility measurements.[21,22] A few NMR studies show amide−Li^{+} interactions via the chemical shift of the carbonyl carbon.[23,24] These studies were performed either in nonaqueous solutions or with molar concentrations of the organic molecules, making quantitative binding information unobtainable. Curiously, a few recent molecular dynamics simulations have concluded that the interactions of cations with amide moieties are actually quite strong.[25−27] For example, Qian and co-workers claimed the association of Na^{+} and K^{+}

Received: December 6, 2012
Published: March 22, 2013

   dx.doi.org/10.1021/ja3119256 | J. Am. Chem. Soc. 2013, 135, 5062−5067

with the amide-containing side chains of poly(*N*-isopropyl acrylamide) (PNIPAM) dominated over the interactions of even the most weakly hydrated anions. In sharp contrast, other MD simulations found that the interactions of anions are indeed dominant.[11,28]

Herein, we have directly tested the association between butyramide, a model amide-containing molecule, and the chloride salts of Na^+, K^+, Li^+, Ca^{2+}, and Mg^{2+}. Experiments were performed in bulk solution by attenuated total reflection Fourier transform infrared (ATR-FTIR) spectroscopy and at the air/water interface by vibrational sum frequency spectroscopy (VSFS). FTIR provides information about contact pair formation, while VSFS reveals complementary information about cation partitioning into the general vicinity of the amide. As such, the nonlinear optical experiments should represent a combination of solvent separated interactions as well as contact pair formation. Both spectroscopies reveal that cation−amide interactions are extremely weak in comparison to anion−amide interactions for I^-, SCN^-, or ClO_4^-. Moreover, the cations follow a direct Hofmeister series. Specifically, strongly hydrated cations bind to the amide carbonyl oxygen at molar salt concentrations, while Na^+ and K^+ do not bind at all (Figure 1).

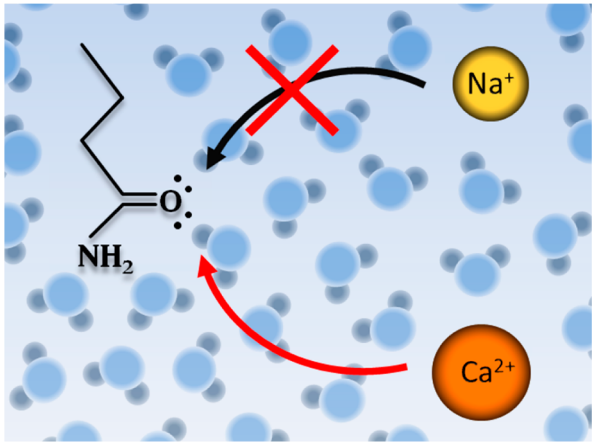

Figure 1. Schematic representation of a butyramide molecule in aqueous medium. The arrows indicate Ca^{2+} can bind to amide oxygen, whereas Na^+ cation cannot.

Data from the amide I band demonstrate that no more than 30% of the carbonyl oxygen sites are paired with metal cations even at 5 M $CaCl_2$. Mg^{2+} and Li^+ interact even more weakly.

MATERIALS AND METHODS

Materials. All inorganic salts (≥99.9%) (from Aldrich, MO and Fisher, NJ) and butyramide (≥99%) were used as received. Aqueous solutions were prepared from purified water with a minimum resistivity of 18.1 MΩ·cm (NANOpure Ultrapure Water System, Barnstead, Dubuque, IA). D_2O samples were prepared with heavy water which was obtained from Cambridge Isotope Laboratories (99.98%, Andover, MA). The *d*-butyramide samples were prepared by dissolving butyramide in D_2O and vacuum drying the samples, which led to the exchange of NH protons by deuterium from the heavy water.[29] This deuterium exchange process was performed a minimum of three times. ATR FTIR samples were prepared by addition of the desired amount of anhydrous salts to a 100 mM *d*-butyramide solution in D_2O. The amide I bands can have contributions from the C−N stretching mode and the NH_2 bending mode as well as the C═O stretch.[30] By performing the experiments in D_2O with fully exchanged ND_2 groups, the overwhelming contribution to the amide I band is just from the C═O stretch. Also, anhydrous high-purity salts (≥99.99%) and heavy water were required to attenuate the interference of the broad water bending peak background in the amide I region. It should be noted that VSFS samples were prepared in H_2O by the addition of the desired amount of salt to 300 mM butyramide in 10 mM Tris-HCl buffer at pH 7.0. In this case, the goal was to monitor the interfacial water OH signal in the presence of a Gibbs monolayer of butyramide.

The VSFS spectra of butyramide were found to be pH independent within experimental error. Water structure at the air/butyramide/water interface was monitored at pH 3.0, 7.0, and 10.0. The acidity of the solutions was adjusted by adding HCl or NaOH to 300 mM butyramide solution. The spectra under these conditions are provided in Figure S1. These results confirmed that neither butyramide nor the interfacial water structure bands could be substantially affected by changing solution pH. In additional control experiments, VSFS experiments in the CH stretch region were also tested in D_2O. The samples were prepared under otherwise identical conditions as for H_2O. These experiments showed the CH peak intensities were little changed under the conditions of the experiments (Figure S2a). VSFS control experiments as a function of butyramide concentration in H_2O (Figure S2b) and in D_2O with 300 mM butyramide in the presence and absence of 4 M metal chloride salts were also investigated (Figure S3). The latter experiments provided evidence for modest changes in monolayer structure or coverage in the presence and absence of salt. There were also some differences between monolayer ordering as a function of cation identity. These differences were relatively small and are discussed in the Supporting Information.

VSFS Measurements. Our VSFS system has been described elsewhere.[31−33] VSFS experiments were performed at room temperature using a 35 mL sample of a 300 mM butyramide solution with the desired salt type and concentration. This was poured into a Langmuir trough (Model 601M, Nima, U.K.). Some butyramide molecules partitioned to the interface to form a Gibbs monolayer under these conditions. A fixed frequency visible beam at 532 nm and a tunable infrared beam were spatially and temporally aligned to the air/butyramide/water interface. All VSFS experiments were performed with the ssp polarization combination (s, sum frequency; s, visible; and p, infrared).

In the present studies, the VSFS spectrum for each sample was taken a minimum of three times. The spectra were collected from 2700 to 3800 cm^{-1}, which covers the CH, OH, and NH stretch regions. The oscillator strength (O.S.) of the water peaks was calculated by fitting the spectra to the following equation by using MATLAB software (version 7.12.0.635):

$$X_{\mathrm{eff}}^{(2)} = X_{\mathrm{NR}}^{(2)} + X_{\mathrm{R}}^{(2)} = X_{\mathrm{NR}}^{(2)} + \sum_q \frac{A_q}{\omega_{\mathrm{IR}} - \omega_q + i\Gamma_q} \quad (1)$$

The frequency-independent nonresonant ($X_{NR}^{(2)}$) and the frequency-dependent resonant ($X_R^{(2)}$) terms are components of the effective second-order nonlinear susceptibly ($X_{eff}^{(2)}$). $X_R^{(2)}$ can be expressed as a sum over the resonant modes, q, that can be tuned to resonance with the input infrared beam (ω_{IR}). Such modes have a resonant frequency (ω_q), a peak width (Γ_q), and an oscillator strength (A_q). The relative phase of each peak was confirmed by employing the maximum entropy method (MEM) to calculate the imaginary part of $X_{eff}^{(2)}$.[34−36] This is discussed in more detail in the Supporting Information.

ATR FTIR Measurements. Infrared spectra were collected with a Nicolet 470 FTIR spectrometer which was equipped with a Pike Miracle ATR attachment that contained a single-bounce ZnSe crystal (Pike Technologies, Madison, WI) and an MCT detector (Thermo Electron Corp., Madison, WI), which was cooled by liquid nitrogen.[37,38] All spectra were collected at 2 cm^{-1} resolution with 256 scans over a window from 1000 to 4000 cm^{-1}. One level of zero filling as well as the Black−Harris apodization function were employed.

Each sample was measured a minimum of three times. Moreover, an otherwise identical salt solution without butyramide was used as a background and measured just before the sample measurement was made. This background was subtracted off from each sample spectrum. Spectral fitting was performed using Origin (version 7.0, Microsoft,

dx.doi.org/10.1021/ja3119256 | J. Am. Chem. Soc. 2013, 135, 5062−5067

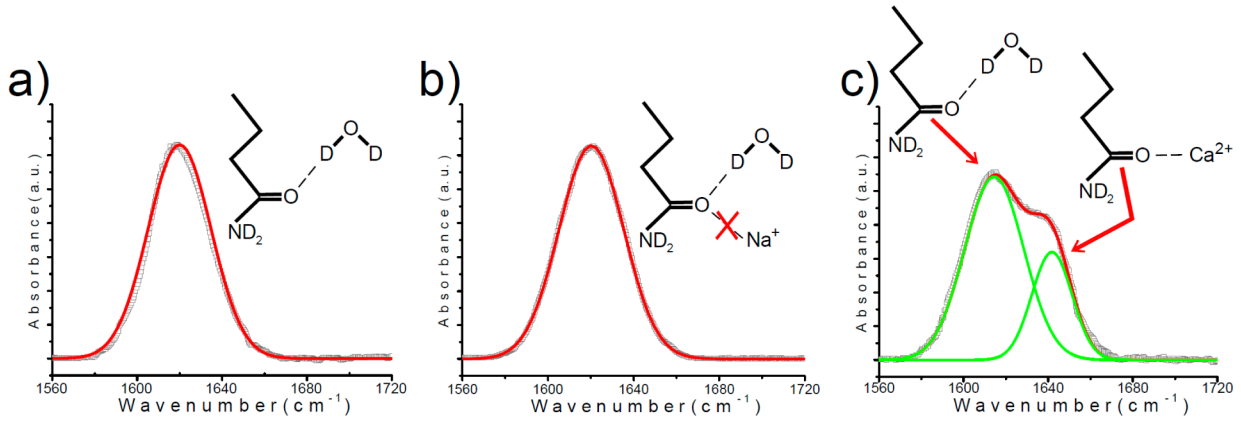

Figure 2. FTIR spectra of the amide I band for *d*-butyramide in (a) D_2O, (b) 5 M NaCl in D_2O, and (c) 5 M $CaCl_2$ in D_2O. The schematic diagrams associated with each spectrum show the type of cation and water interactions with the amide in each case. The gray circles represent the FTIR spectral data, and the red lines are the overall fits to the data. For (c), green curves are also provided showing the two individual Gaussians fits to the overall spectrum.

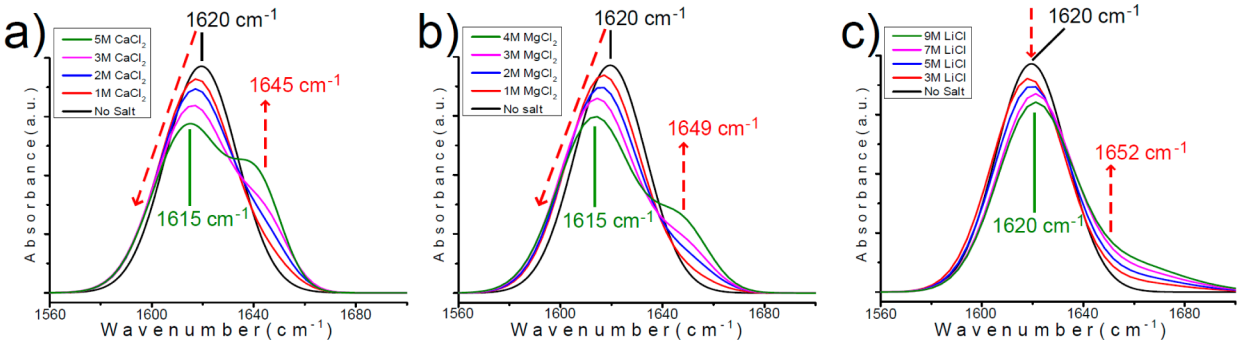

Figure 3. FTIR spectra of the amide I band for *d*-butyramide at (a) $CaCl_2$ concentrations from 0 to 5 M, (b) $MgCl_2$ from 0 to 4 M, and (c) LiCl from 0 to 9 M.

Northampton, MA). The number of Gaussian peaks required to fit a given spectrum was determined using a second derivative test.[39] The least error sum method was employed to check the quality of the spectral fitting, and all spectral fits shown here have the lowest least error sum.

RESULTS

ATR-FTIR Measurements of *d*-Butyramide. Figure 2 shows the amide I band from *d*-butyramide in (a) pure D_2O, (b) a solution containing 5 M NaCl, and (c) a solution containing 5 M $CaCl_2$. The spectra with 5 M NaCl and without any salt gave rise to a single peak at 1620 cm^{-1} that showed no variation in intensity with increasing concentration of the sodium salt. This peak could easily be fit by a single Gaussian curve. By contrast, the amide I band split into two distinct resonances with 5 M $CaCl_2$. These could be fit by two separate Gaussian curves at 1615 and 1645 cm^{-1} with the lower frequency peak showing a slight red-shift from the pure D_2O case. In fact, this peak continuously red-shifted and decreased in intensity as $CaCl_2$ was added to solution (Figure 3a). The higher frequency peak did not appear to show a frequency shift but continuously rose in intensity as $CaCl_2$ was added.

Amide bands consist of a combination of the carbonyl stretch, the NH bend, and the CN stretch. However, the amide I band from small molecules, like butyramide, arises almost exclusively from the carbonyl stretch in D_2O and appears at 1620 cm^{-1}.[30] By contrast, the same amide I band appears at 1715 cm^{-1} in air or vacuum.[40] The red-shift in water compared with air can be explained by the hydrogen bonding of water molecules to the organic molecule. The amide I band will also red-shift relative to air when bonded to the NH of urea,[41] the NH of another amide,[16,42] or through contact pairing with a metal ion.[16,17] However, these latter red shifts are almost always smaller than the one for water, which involves significant charge transfer to the σ^* orbital of water's OH bond.[43] As a consequence, the amide I band appears to blue-shift in bulk aqueous solution upon interaction with most species other than water. For metal ions, this phenomenon is not limited to amides. For example, the CN stretch of thiocyanate[44,45] and the carbonyl stretch of acetone[46] both show a blue-shift in aqueous solution when a divalent metal ion displaces water to form a contact pair. As such, the higher frequency peak in Figure 2c can be assigned to a contact pair between Ca^{2+} and the amide, while the lower frequency peak should represent the water bonded species. Indeed, these assignments are consistent with the increasing intensity of the higher frequency peak, and the attenuation of the lower frequency peak as salt is added to solution. The slight red-shift of the lower frequency peak with salt concentration may be caused by increasing interactions of Ca^{2+} with oxygen atoms from water molecules in the amide's hydration shell. It should be noted, however, that the dielectric constant of water changes from 78.5 to 49 as the $CaCl_2$ concentration is increased from 0 to 4M,[47,48] which may also influence the peak position of the water-bonded amide.

Data analogous to that of $CaCl_2$ for the amide I spectra of *d*-butyramide is shown for $MgCl_2$ and LiCl at various

dx.doi.org/10.1021/ja3119256 | J. Am. Chem. Soc. 2013, 135, 5062−5067

concentrations (Figure 3b,c). Once again, the higher frequency peak rose in intensity while the 1620 cm^{-1} fell and red-shifted for Mg^{2+} and only fell for Li^+. The higher frequency peak occurred at 1649 cm^{-1} with 4 M $MgCl_2$ and 1652 cm^{-1} with 9 M LiCl. The slightly higher frequency blue shift for the Li^+–amide interaction is consistent with more modest amide bond polarization. Additional data for the amide I band was collected in the presence of KCl as a function of concentration. As with NaCl, no evidence was found within experimental error for either a frequency shift or an intensity change of the amide I band peak at 1620 cm^{-1} even with a saturation concentration of KCl (see Supporting Information).

The salt concentration dependence of the FTIR peaks in Figure 3 can be employed to obtain quantitative data about the fraction of metal ions in direct contact with the amide oxygen. This is done by plotting the ratio of the area under the high-frequency peak to the total area under the amide I band at various salt concentrations (Figure 4). As can be seen, the

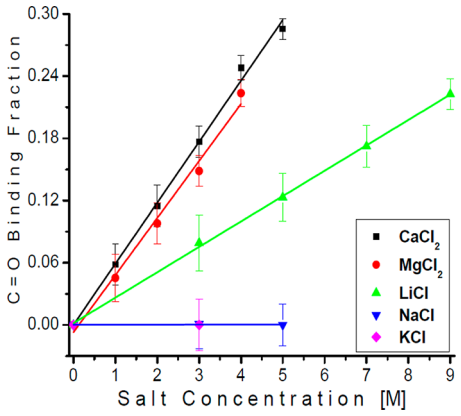

Figure 4. Binding fraction of metal bound amide vs total amide concentration for five different salts.

fraction of contact pairs between metal ions and amides rose linearly with increasing concentrations of $CaCl_2$, $MgCl_2$, and LiCl. The slopes were considerably steeper for the divalent cations compared with LiCl, and the slope for Ca^{2+} was slightly steeper (more favorable binding) compared with Mg^{2+}. Since, NaCl and KCl led to no observable peak splitting or shifts, their binding fractions should be zero under all conditions. Such data are in good agreement with a direct cationic Hofmeister series, although some series report Mg^{2+} rather than Ca^{2+} as the strongest salting-in agent:[45,46]

$$Ca^{2+} > Mg^{2+} > Li^+ > Na^+ \approx K^+$$

The data in Figure 4 cannot be employed to directly abstract equilibrium dissociation constant information, since even Ca^{2+} simply does not bind tightly enough to get beyond the linear portion of the binding curve by saturation concentration. Nevertheless, nearly 30% of the carbonyl oxygen binding sites were occupied at 5 M $CaCl_2$. If one extrapolates from this value to the concentration at which 50% of the sites would be occupied by Ca^{2+}, an approximation of the apparent K_d value of 8.5 M would be obtained. By analogy, the apparent K_d values would be 9.5 M for Mg^{2+} and 20.2 M for Li^+. All these values are beyond the saturation concentrations of the respective salts and therefore hypothetical. Moreover, they are sufficiently weak that they border on being merely statistical. For favorable binding, the contact pairing energy gain must more than offset the energy cost of shedding the hydration layers of both the carbonyl oxygen and the metal ions. Specifically, the free energies of the carbonyl–water, carbonyl–cation, cation–water, and water–water interactions are all involved. It should also be noted that contact pair formation for both Na^+ and K^+ are unfavorable and are, as such, depleted from the amide carbonyl oxygen/water interface.

VSFS Measurements of Butyramide. FTIR of the amide I band primarily provides information on contact pair formation between metal ions and the carbonyl oxygen of the amide. Therefore, it is important to use a complementary spectroscopy to glean information on the overall partitioning of cations to the amide interface. VSFS can provide such information as long as one ion preferentially partitions to the amide/water interface.[49,50] This will be the case for metal ions in chloride solutions, as chloride interactions with the amides are negligible.[49] Figure 5 shows the VSFS spectra of the air/

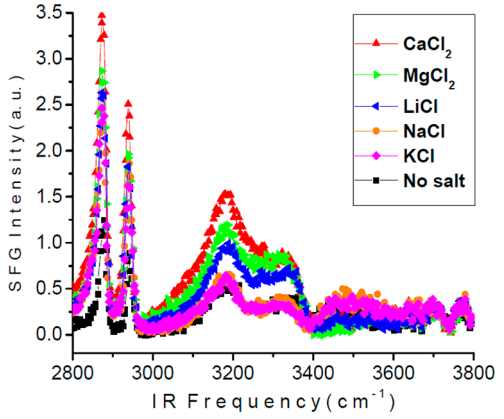

Figure 5. VSFS spectra for Gibbs monolayers of butyramide at the air/water interface. For each spectrum the subphase contained 4 M of the respective salt as indicated in the legend. The one exception was KCl, which was measured in a saturated solution (~3.8 M).

butyramide/water interface with 4 M chloride salt solutions of Ca^{2+}, Mg^{2+}, Li^+, Na^+, 3.8 M K^+, and pure H_2O in the subphase. The two dominant peaks in the CH range at 2880 and 2940 cm^{-1} correspond to the CH_3 symmetric stretch and a Fermi resonance, respectively.[33,51] On the other hand, the water region (3100–3600 cm^{-1}) appears to look unusual compared with literature spectra.[49,52−55] In fact, four bands can be identified. The two broadest, around 3200 and 3420 cm^{-1}, correspond to the usual assignments of more-ordered and less-ordered interfacial water structure, respectively. However, two relatively sharp peaks are also found near 3180 and 3390 cm^{-1}. These resonances are caused by the symmetric and asymmetric NH_2 stretch modes.[56] The lower frequency NH_2 resonance constructively interferes with the water bands, whereas the higher frequency peak interferes destructively and leads to a dip in the spectrum (see Supporting Information for details concerning peak fitting). The presence of different salts in the subphase strongly affected the water orientation. Indeed, the adsorption of cations should cause net water orientation with the OH group facing toward the butyramide monolayer in agreement with other interfacial ion adsorption studies.[49,52] Moreover, a greater degree of cation adsorption over its counterion should correspond to increased water ordering.[49,50] Indeed, the presence of 4 M $CaCl_2$ and $MgCl_2$ in the subphase dramatically enhances the intensity of the OH stretch peaks,

dx.doi.org/10.1021/ja3119256 | J. Am. Chem. Soc. 2013, 135, 5062−5067

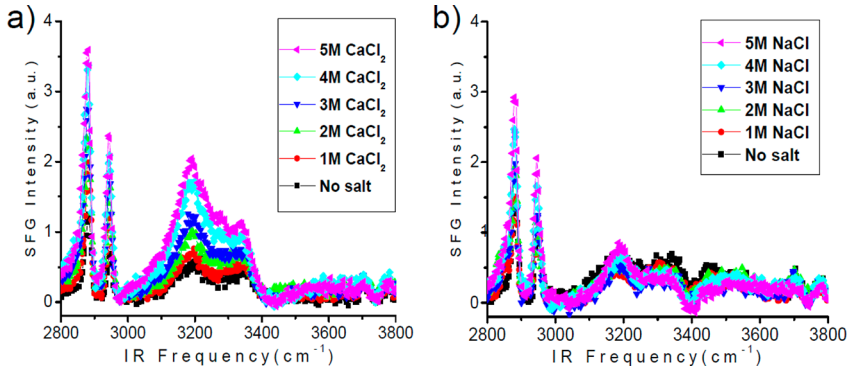

Figure 6. VSFS spectra of the air/butyramide/water interface as a function of (a) $CaCl_2$ and (b) NaCl concentrations.

whereas 4 M LiCl leads to more moderate water signal enhancement. By contrast, the presence of 4 M NaCl and 3.8 M KCl hardly perturbs the water structure within experimental error. The order of the intensity enhancements for the 3200 and 3420 cm^{-1} peaks closely track the cationic Hofmeister series observed for the FTIR data (Figures 2−4).

VSFS spectra of air/butyramide water interface as a function of $CaCl_2$ and NaCl concentrations are shown in Figure 6a,b, respectively. The water structure peaks increase continuously as a function of $CaCl_2$ concentration, whereas almost no effect is observed by adding NaCl to the subphase up to the saturation point. $MgCl_2$ and LiCl solutions showed behavior similar to $CaCl_2$, while addition of KCl to the subphase led to no appreciable change in the water spectrum (see Figure S10).

In order to obtain more quantitative information, the VSFS spectra need to be fit to eq 1 in order to obtain the oscillator strength for the water bands. Figure 7 provides the O.S.

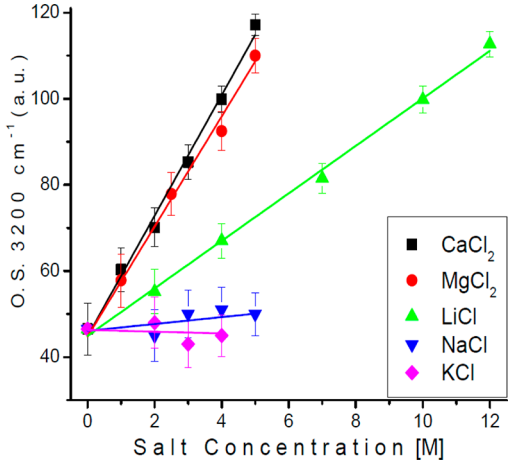

Figure 7. Oscillator strength of 3200 cm^{-1} peak as a function of different salt concentrations in the subphase.

strength values for the 3200 cm^{-1} peak as a function of salt concentration for the five chloride salts. Linear increasing trends are observed for Ca^{2+}, Mg^{2+}, and Li^+ cations with the same ordering in slopes as found with FTIR in Figure 4. Such close agreement is remarkable because the VSFS data report on interfacial water structure ordering, while the FTIR data correspond to the carbonyl stretch of the amide moiety in bulk solution. Also, the Na^+ and K^+ cations showed negligible changes in their 3200 cm^{-1} O.S. values. Again, this is in good agreement with the FTIR data. Such results confirm that the free energy of partitioning Na^+ and K^+ to an amide-containing monolayer is unfavorable. It should be noted that essentially the same results as reported in Figure 7 can be found by plotting the O.S. of the 3420 cm^{-1} against the salt concentration instead of the 3200 cm^{-1} peak.

DISCUSSION AND CONCLUSION

In proteins, the driving force for cation−polypeptide interactions should generally involve electrostatic interactions between negatively charged carboxylate side chains and cations.[57−61] Such interactions can be far tighter than anion−peptide backbone interactions and even dominate the phase behavior of a protein under appropriate conditions.[58] As shown above, however, the interactions of cations with amides are extremely weak with Ca^{2+} giving rising to the tightest apparent binding. By contrast, the measured K_d values for weakly hydrated anions with their respective peptide binding sites are substantially tighter. For example, SCN^- yields an apparent K_d value of ∼200 mM in various spectroscopic and thermodynamic measurements.[49,62] Thus, anion affinity for amide binding sites is nearly 2 orders of magnitude tighter compared with the most strongly interacting cations (e.g., Ca^{2+} vs SCN^-). Furthermore, the nature of cation and anion binding for uncharged polypeptide backbones is significantly different. Indeed, strongly hydrated cations tend to bind, whereas only the most weakly hydrated anions accumulate around protein backbones.[11,28,63] This difference in Hofmeister series properties can be understood in light of the very different binding sites for cations and anions. As noted in the Introduction, the amide oxygen is the key binding site for cations. By contrast, the binding site for Hofmeister anions to peptide backbones involves a combination of the amide nitrogen and the adjacent hydrophobic methylene unit.[11]

Both Na^+ and K^+ are known to bind with model amide molecules/polypeptides in the gas phase.[64,65] The situation in aqueous solutions is different. In the absence of metal ion binding, the amide oxygen should hydrogen bond to water, and the cation will be surrounded by its hydration shell. These interactions need to be at least partially disrupted in order for cation−amide contact pairing to take place. Herein, we have shown spectroscopic evidence for very weak binding behavior for Ca^{2+} and Mg^{2+}, nearly statistical binding for Li^+, and exclusion for Na^+ and K^+ from the amide oxygen. Until now, molecular dynamics simulations have found evidence for varying degrees of binding of Na^+ and K^+ cations with the amide oxygen in aqueous solutions.[11,25−28] Such differences among the simulations presumably reflect the challenges associated with accounting for the very small differences in

dx.doi.org/10.1021/ja3119256 | J. Am. Chem. Soc. 2013, 135, 5062−5067

free energy values associated with the bound and unbound states. Nevertheless, simulations that find tight associations between metal cations and the carbonyl oxygen of amides are not consistent with the spectroscopic data.

■ ASSOCIATED CONTENT

Supporting Information

VSFS spectra of butyramide on salt solutions at various pH values and also at different salt types and concentrations in water and D_2O solvated media. The ATR FT-IR spectra and Gaussian fittings of *d*-butyramide at different salt identity and concentrations in D_2O-solvated media. This material is available free of charge via Internet at http://pubs.acs.org.

■ AUTHOR INFORMATION

Corresponding Author

psc11@psu.edu

Notes

The authors declare no competing financial interest.

■ ACKNOWLEDGMENTS

This work was supported by the National Science Foundation (CHE-0094332) and the Robert A. Welch Foundation (A-1421).

■ REFERENCES

(1) Hofmeister, F. *Arch. Exp. Pathol. Pharmakol.* **1888**, *24*, 247.
(2) Collins, K. D.; Washabaugh, M. W. *Q. Rev. Biophys.* **1985**, *18*, 323.
(3) Cacace, M. G.; Landau, E. M.; Ramsden, J. J. *Q. Rev. Biophys.* **1997**, *30*, 241.
(4) Kunz, W.; Lo Nostro, P.; Ninham, B. W. *Curr. Opin. Colloid Interface Sci.* **2004**, *9*, 1.
(5) Kalcher, I.; Horinek, D.; Netz, R. R.; Dzubiella, J. *J. Phys.: Condens. Matter* **2009**, 21.
(6) Zhang, Y. J.; Cremer, P. S. *Annu. Rev. Phys. Chem.* **2010**, *61*, 63.
(7) Traube, J. *J. Phys. Chem.* **1910**, *14*, 452.
(8) Baldwin, R. L. *Biophys. J.* **1996**, *71*, 2056.
(9) Melander, W.; Horvath, C. *Arch. Biochem. Biophys.* **1977**, *183*, 200.
(10) Collins, K. D. *Biophys. Chem.* **2006**, *119*, 271.
(11) Rembert, K. B.; Paterova, J.; Heyda, J.; Hilty, C.; Jungwirth, P.; Cremer, P. S. *J. Am. Chem. Soc.* **2012**, *134*, 10039.
(12) Coates, J. P. *Appl. Spectrosc. Rev.* **1996**, *31*, 179.
(13) Von Hippel, P. H.; Peticola, V.; Schack, L.; Karlson, L. *Biochemistry* **1973**, *12*, 1256.
(14) Bykov, S.; Asher, S. *J. Phys. Chem. B* **2010**, *114*, 6636.
(15) Harding, M. M. *Acta Crystallogr., Sect. D: Biol. Crystallogr.* **2004**, *60*, 849.
(16) Balasubramanian, D.; Shaikh, R. *Biopolymers* **1973**, *12*, 1639.
(17) Bonner, O. D.; Jordan, C. F. *Physiol. Chem. Phys.* **1976**, *8*, 293.
(18) Bello, J.; Bello, H. R. *Nature* **1962**, *194*, 681.
(19) Bello, J.; Haas, D.; Bello, H. R. *Biochemistry* **1966**, *5*, 2539.
(20) Bello, J.; Bello, H. R. *Nature* **1961**, *190*, 440.
(21) Nandi, P. K.; Robinson, D. R. *J. Am. Chem. Soc.* **1972**, *94*, 1308.
(22) Nandi, P. K.; Robinson, D. R. *J. Am. Chem. Soc.* **1972**, *94*, 1299.
(23) Adams, M. J.; Baddiel, C. B. *J. Chem. Soc., Faraday Trans.* **1975**, *71*, 1823.
(24) Rao, C. P.; Balaram, P.; Rao, C. N. R. *J. Chem. Soc., Faraday Trans.* **1980**, *76*, 1008.
(25) Du, H. B.; Wickramasinghe, R.; Qian, X. H. *J. Phys. Chem. B* **2010**, *114*, 16594.
(26) Heyda, J.; Vincent, J. C.; Tobias, D. J.; Dzubiella, J.; Jungwirth, P. *J. Phys. Chem. B* **2010**, *114*, 1213.
(27) Ioannou, F.; Archontis, G.; Leontidis, E. *J. Phys. Chem. B* **2011**, *115*, 13389.
(28) Algaer, E. A.; van der Vegt, N. F. A. *J. Phys. Chem. B* **2011**, *115*, 13781.
(29) Maeda, Y.; Higuchi, T.; Ikeda, I. *Langmuir* **2000**, *16*, 7503.
(30) Barth, A.; Zscherp, C. *Q. Rev. Biophys.* **2002**, *35*, 369.
(31) Kim, G.; Gurau, M. C.; Lim, S. M.; Cremer, P. S. *J. Phys. Chem. B* **2003**, *107*, 1403.
(32) Kataoka, S.; Gurau, M. C.; Albertorio, F.; Holden, M. A.; Lim, S. M.; Yang, R. D.; Cremer, P. S. *Langmuir* **2004**, *20*, 1662.
(33) Kataoka, S.; Cremer, P. S. *J. Am. Chem. Soc.* **2006**, *128*, 5516.
(34) Sovago, M.; Vartiainen, E.; Bonn, M. *J. Phys. Chem. C* **2009**, *113*, 6100.
(35) Sagle, L. B.; Cimatu, K.; Litosh, V. A.; Liu, Y.; Flores, S. C.; Chen, X.; Yu, B.; Cremer, P. S. *J. Am. Chem. Soc.* **2011**, *133*, 18707.
(36) de Beer, A. G. F.; Samson, J. S.; Hua, W.; Huang, Z. S.; Chen, X. K.; Allen, H. C.; Roke, S. *J. Chem. Phys.* **2011**, *135*, 224701.
(37) Batchelor, J. D.; Olteanu, A.; Tripathy, A.; Pielak, G. J. *J. Am. Chem. Soc.* **2004**, *126*, 1958.
(38) Omta, A. W.; Kropman, M. F.; Woutersen, S.; Bakker, H. J. *Science* **2003**, *301*, 347.
(39) Snedecor, G. W. C. W. G. *Statistical Methods*; 8th ed.; Iowa State University Press: Ames, IA, 1989.
(40) Balasubr., D.; Shaikh, R. *Biopolymers* **1973**, *12*, 1639.
(41) Sagle, L. B.; Zhang, Y. J.; Litosh, V. A.; Chen, X.; Cho, Y.; Cremer, P. S. *J. Am. Chem. Soc.* **2009**, *131*, 9304.
(42) Maeda, Y.; Nakamura, T.; Ikeda, I. *Macromolecules* **2002**, *35*, 10172.
(43) Reed, A. E.; Curtiss, L. A.; Weinhold, F. *Chem. Rev.* **1988**, *88*, 899.
(44) Park, S.; Ji, M. B.; Gaffney, K. J. *J. Phys. Chem. B* **2010**, *114*, 6693.
(45) Anticjovanovic, A.; Jeremic, M.; Lalic, M.; Long, D. A. *J. Raman Spectrosc.* **1989**, *20*, 523.
(46) Lalic, M.; AnticJovanovic, A.; Jeremic, M.; Sasic, S. *Spectrosc. Lett.* **1996**, *29*, 267.
(47) Schrier, E. E.; Schrier, E. B. *J. Phys. Chem.* **1967**, *71*, 1851.
(48) Harris, F. E.; Okonski, C. T. *J. Phys. Chem.* **1957**, *61*, 310.
(49) Chen, X.; Yang, T.; Kataoka, S.; Cremer, P. S. *J. Am. Chem. Soc.* **2007**, *129*, 12272.
(50) Gurau, M. C.; Lim, S. M.; Castellana, E. T.; Albertorio, F.; Kataoka, S.; Cremer, P. S. *J. Am. Chem. Soc.* **2004**, *126*, 10522.
(51) Lu, R.; Gan, W.; Wu, B. H.; Zhang, Z.; Guo, Y.; Wang, H. F. *J. Phys. Chem. B* **2005**, *109*, 14118.
(52) Gragson, D. E.; McCarty, B. M.; Richmond, G. L. *J. Am. Chem. Soc.* **1997**, *119*, 6144.
(53) Gragson, D. E.; Richmond, G. L. *J. Phys. Chem. B* **1998**, *102*, 3847.
(54) Du, Q.; Superfine, R.; Freysz, E.; Shen, Y. R. *Phys. Rev. Lett.* **1993**, *70*, 2313.
(55) Shen, Y. R.; Ostroverkhov, V. *Chem. Rev.* **2006**, *106*, 1140.
(56) Evans, J. C. *J. Chem. Phys.* **1954**, *22*, 1228.
(57) Vrbka, L.; Vondrasek, J.; Jagoda-Cwiklik, B.; Vacha, R.; Jungwirth, P. *Proc. Natl. Acad. Sci. U.S.A.* **2006**, *103*, 15440.
(58) Kherb, J.; Flores, S. C.; Cremer, P. S. *J. Phys. Chem. B* **2012**, *116*, 7389.
(59) Manning, G. S. *Q. Rev. Biophys.* **1978**, *11*, 179.
(60) Dudev, T.; Lim, C. *Chem. Rev.* **2003**, *103*, 773.
(61) Hess, B.; van der Vegt, N. F. A. *Proc. Natl. Acad. Sci. U.S.A.* **2009**, *106*, 13296.
(62) Zhang, Y. J.; Furyk, S.; Bergbreiter, D. E.; Cremer, P. S. *J. Am. Chem. Soc.* **2005**, *127*, 14505.
(63) Chen, X.; Flores, S. C.; Lim, S. M.; Zhang, Y. J.; Yang, T. L.; Kherb, J.; Cremer, P. S. *Langmuir* **2010**, *26*, 16447.
(64) Tsang, Y.; Siu, F. M.; Ho, C. S.; Ma, N. L.; Tsang, C. W. *Rapid Commun. Mass Spectrom.* **2004**, *18*, 345.
(65) Klassen, J. S.; Anderson, S. G.; Blades, A. T.; Kebarle, P. *J. Phys. Chem.* **1996**, *100*, 14218.